5.3

INDO-PACIFIC OCEAN RESPONSE TO INTRASEASONAL FORCING

Duane E. Waliser[1]
Marine Sciences Research Center, State University of New York, Stony Brook, NY

Ragu Murtugudde
Earth System Science Interdisciplinary Center, University of Maryland, College Park, MD

1. INTRODUCTION

We are employing the Gent & Cane ocean general circulation model (GC-OGCM; Gent and Cane, 1989) along with observed high-frequency forcing fields to investigate the role intraseasonal forcing [e.g., Madden-Julian Oscillation; Madden and Julian, 1994], plays in the circulation and thermodynamic structure of the Indo-Pacific Ocean. Our version of the GC-OGCM (cf. Murtugudde et al. 1996; 1998) explicitly accounts for mixed-layer processes (Chen et al. 1994) and upper ocean hydrology, contains a representation of the Indonesian Throughflow, and includes some aspects of the feedback from sea surface temperature (SST) onto the surface fluxes via an atmospheric advective mixed-layer model (Seager et al. 1995). Using composites of the tropical intraseasonal forcing events based on satellite-derived values of wind, rainfall, and surface shortwave forcing, we are exploring the detailed response of the Indo-Pacific warm-pool region to tropical intraseasonal variability (TISV). This includes examining the rectification of the intraseasonal time scale to longer time scales and/or the mean state, the relative roles of the different forcing components on the response, the nature of the recovery mechanisms of the ocean to one or more TISV events, how the modulation of high frequency forcing by TISV influences the ocean response, the modulation of the Indonesian throughflow, etc. The results reported here address the first two of these issues.

2. FORCING DATA

Ocean forcing data includes daily surface winds derived from SSM/I (Atlas et al. 1996), daily surface shortwave values from ISCCP (Bishop et al. 1997), and 5-day rainfall values from CMAP (Xie and Arkin, 1997). The surface wind values are used to compute stresses and wind speed, the latter of which is used in the atmospheric advective mixed model to compute turbulent fluxes. Each of the above data sets is used to form climatological forcing data sets used for the "climatological" simulations. Note that a low wind threshold (>= 4m/s) is applied to the climatological wind speed forcing to account for unresolved high frequency wind variability. In addition, the high frequency components of these data sets are used to construct composite TISV forcing events that are added to the climatological forcing for the TISV simulations.

3. COMPOSITE TISV FORCING

TISV events are identified through extended EOF (EEOF) analysis of bandpassed (35-90 days) rainfall data. Given that TISV has a strong seasonal dependence in this region (e.g., Wang and Rui, 1995), with the eastward-propagating mode of TISV favored in boreal winter and the northeast-propagating mode favored in boreal summer, our examination discriminates between these two seasons/modes. This is done by first separating the data by season, with "winter" extending between Nov-Apr and "summer" extending between May-Oct. EEOFs are computed for +/- 7 pentad time lags on the region between 30ºE and 180ºE for each season. For each season, modes 1 and 2 represent a "pair" of modes, each accounting for about 10% of the variance, which when considered together represent a traveling "wave-like" structure with about a 50 day period. TIVS events are selected from the unit normalized amplitude time series of mode 1 when the value exceeds 1.5. The selected TISV events are then averaged to form a composite forcing structure. These composite forcing fields are then multiplied by a scale factor (in this case 2) to account for the decreased magnitudes of the signal associated with the averaging process. The above produces a "typical" TISV event for each forcing field (e.g., Wellter and Anderson, 1996). For the TISV simulations, the above perturbation forcing fields are added to the climatological. In addition, since the above forcing structures exhibit a cyclic structure, any number of them can be concatenated together to represent an idealized sequence of TISV events. Figure 1 shows the TISV forcing for a sequence of three events. Note that for the case of the wind speed, the anomaly is added to the climatological forcing without additional application of the low wind speed threshold. Thus for the suppressed (wind speed) phase of TISV, the wind speed can and does fall below the climatological threshold (>=4m/s; cf. Weller and Anderson, 1996).

4.RESULTS

To examine the influence of the above idealized intraseasonal forcing on the upper ocean in the Indo-Pacific region, the GC-OGCM was integrated for 15 years from an initial condition based on Levitus (1994) using climatological forcing and a resolution of 1/3º x 1/2º (lat x lon) with 15 sigma layers. This led to a near-surface thermal and dynamic "steady state. From this state, the above intraseasonal perturbation forcing was added to the climatological forcing. In the case of the winter (summer; not shown) mode, the perturbation forcing included three events starting in the months of November (May). Results for the winter case are presented in Figure 2 in terms of the departure in the ocean's SST response from the use of climatological forcing alone.

The upper left panel of Figure 2 illustrates the influence of the intraseasonal forcing on SST averaged

[1]Corresponding author address: Duane E. Waliser, Marine Sciences Research Center, State University of New York, Stony Brook, NY, 11794-5000; duane.waliser@sunysb.edu.

between 5ºN and 5ºS (hereafter All-Forcing case). The vertical axis indicates time since the intraseasonal perturbations were added to the climatological forcing. Note that the imposed sequence of three intraseasonal forcing events occur during the first 5 to 6 months shown with the remaining "adjustment" period consisting of climatological forcing alone. Evident in the Indian and western Pacific Ocean are the fairly well defined eastward propagating intraseasonal oscillations in SST. These oscillations have peak-to-peak amplitudes of about 1.0ºC, roughly consistent with the observational results of Waliser (1996) and Jones et al. (1998). Of interest in the present study is the low-frequency rectification of the intraseasonal forcing. Applying a low-pass filter in time (not shown) indicates that the application of intraseasonal forcing leads to a slight warming (~0.4 C) in the western Pacific during the period of active TISV forcing with a neutral influence to weak warming in the Indian Ocean. However, the latter appears to have an evolving nature in which each successive TISV event has a slightly cooler negative SST anomaly, with the whole perturbation structure appearing to move eastward. This might be the result of the positive longitudinal SST gradient in this region, which in conjunction with westerly wind bursts might lead to cooler water being advected farther east with each successive TISV event.

The result of a warming influence from TISV in the western Pacific is at odds with the results of Kessler and Kleeman (2000). Their study employed a Tropical Pacific version of the Gent-Cane ocean model to study the low-frequency rectification of the TISV. Based on idealized, analytic TISV forcing that does not include buoyancy perturbations associated with rainfall or radiation, they concluded that the TISV forcing leads to a weak cooling (~0.4ºC) in the western Pacific Ocean. The difference in these two results appears to result at least in part from the neglect of the buoyancy forcing terms as well as the application of an absolute low-wind speed threshold (>=4m/s), i.e. one that is independent of the phase of the oscillation. The upper right panel of Figure 1 shows our CG-OGCM result when the composite TISV perturbations associated with rainfall and shortwave are not included in the anomalous TISV forcing. Apparent is the decrease in the low-frequency warming that was evident in the All-Forcing case. The lower left panel shows the result when in addition to removing the buoyancy perturbations, an absolute critical wind speed threshold is employed (=4m/s). This absolute threshold prevents the suppression of sensible and latent heat flux anomalies that normally enhance the warming during the low wind speed phases of the oscillation. Examination of this case shows that the original intraseasonal warming signatures in the All-Forcing case are nearly absent, leading in this case to a low-frequency cooling, a result that is very consistent with Kessler and Kleeman (2000). The above results in conjunction with observational analogs, as well as the the N. H. summer case(s) will be discussed in the oral presentation.

References

Atlas R., R. H. Hoffman, S. C. Bloom, J. C. Jusem, J. Ardizzone. 1996: A multiyear global surface wind velocity dataset using SSM/I wind observations. Bull. Amer. Met. Soc. 77, 869-882.

Bishop, J. K. B., W. B. Rossow and E. G. Dutton, 1997: Surface Solar Irradiance from ISCCP 1983-1991, J. Geophys. Res., 102: (D6) 6883-6910.

Chen, D., L. M. Rothstein, and A. J. Busalacchi, 1994: A hybrid vertical mixing scheme and its application to tropical ocean models, J. Phys. Oceanogr., 10, 2156-2179.

Gent, P., and M. A. Cane, 1989: A Reduced Gravity, Primitive Equation Model of the Upper Equatorial Ocean. J. Comp. Phys., 81, 444-480.

Jones, C., D. E. Waliser, and C. Gautier, 1998: The influence of the Madden and Julian Oscillation on ocean surface heat fluxes and sea surface temperatures. J. Climate, 11, 1057–1072.

Kessler, W. S. and R. Kleeman, 2000: Rectification of the Madden-Julian Oscillation into the ENSO cycle. J. Clim., In Press.

Levitus, S., 1994: Climatological Atlas of the World Ocean. NOAA Prof. Pap. No. 13, U. S. Gov't. Priniting Office.

Madden, R. A., and P. R. Julian, 1994: Observations of the 40-50 day tropical oscillation: A review. Mon. Wea. Rev., 112, 814-837.

Murtugudde, R., R. Seager and A. Busalacchi, 1996: Simulation of the Tropical Oceans with an Ocean GCM Coupled to an Atmospheric Mixed Layer Model. J. Clim., 9, 1795-1815.

Murtugudde, R., A. J. Busalacchi, and J. Beauchamp, 1998: Seasonal to interannual effects of the Indonesian throughflow on the tropical Indo-Pacific basin. J. Geophys. Res., 103, 21,425-21,441.

Seager, R., B. Blumenthal, and Y. Kushnir, 1995: An advective atmospheric mixed layer model for ocean modeling purposes: Global simulation of surface heat fluxes. J. Clim., 8, 1951-1964.

Waliser, D. E., 1996: Formation and Limiting Mechanism for Very High SST: Linking the Dynamics and Thermodynamics. J. Climate, 9, 161-188.

Wang, B., and H. Rui, 1990: Synoptic climatology of transient tropical intraseasonal convection anomalies. Meteor. Atmos. Phys., 44, 43-61.

Weller, R. A. and S. A. Anderson, 1996: Temporal variability and mean values of the surface meteorology and air-sea fluxes in the western equatorial Pacific warm pool during TOGA COARE, J. Climate, 9, 1959-1990.

Xie, P., and P. A. Arkin, 1997: Global Precipitation: A 17-year monthly analysis based on gauge observations, satellite estimates, and numerical model outputs. Bull. Am. Meteor. Soc., 78, 2539-2558.

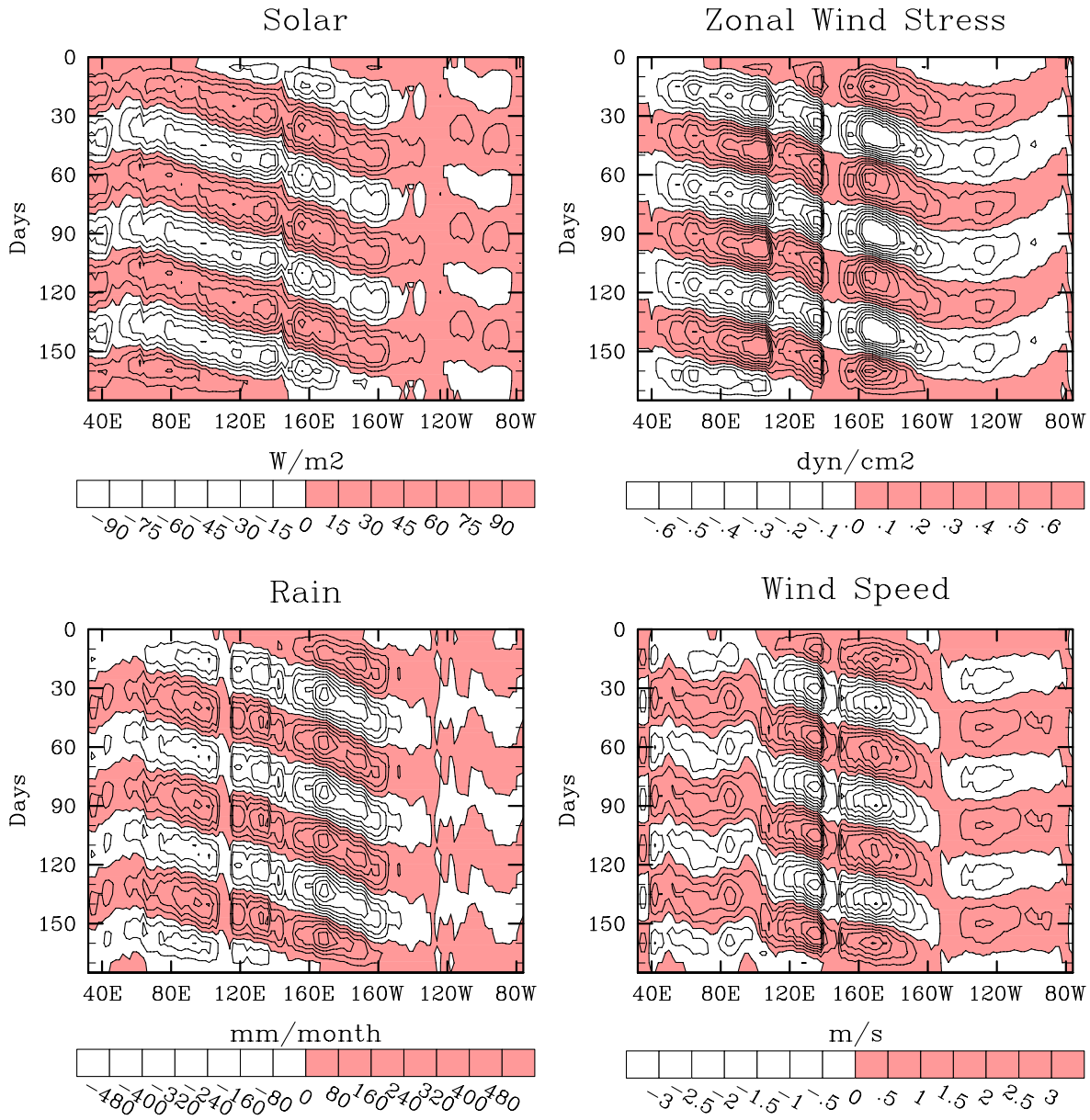

Figure 1. Equatorial (9N-9S) time-longitude diagrams of composite intraseasonal ocean forcing for a sequence of three events. See text for a description of data sources and compositing methods.

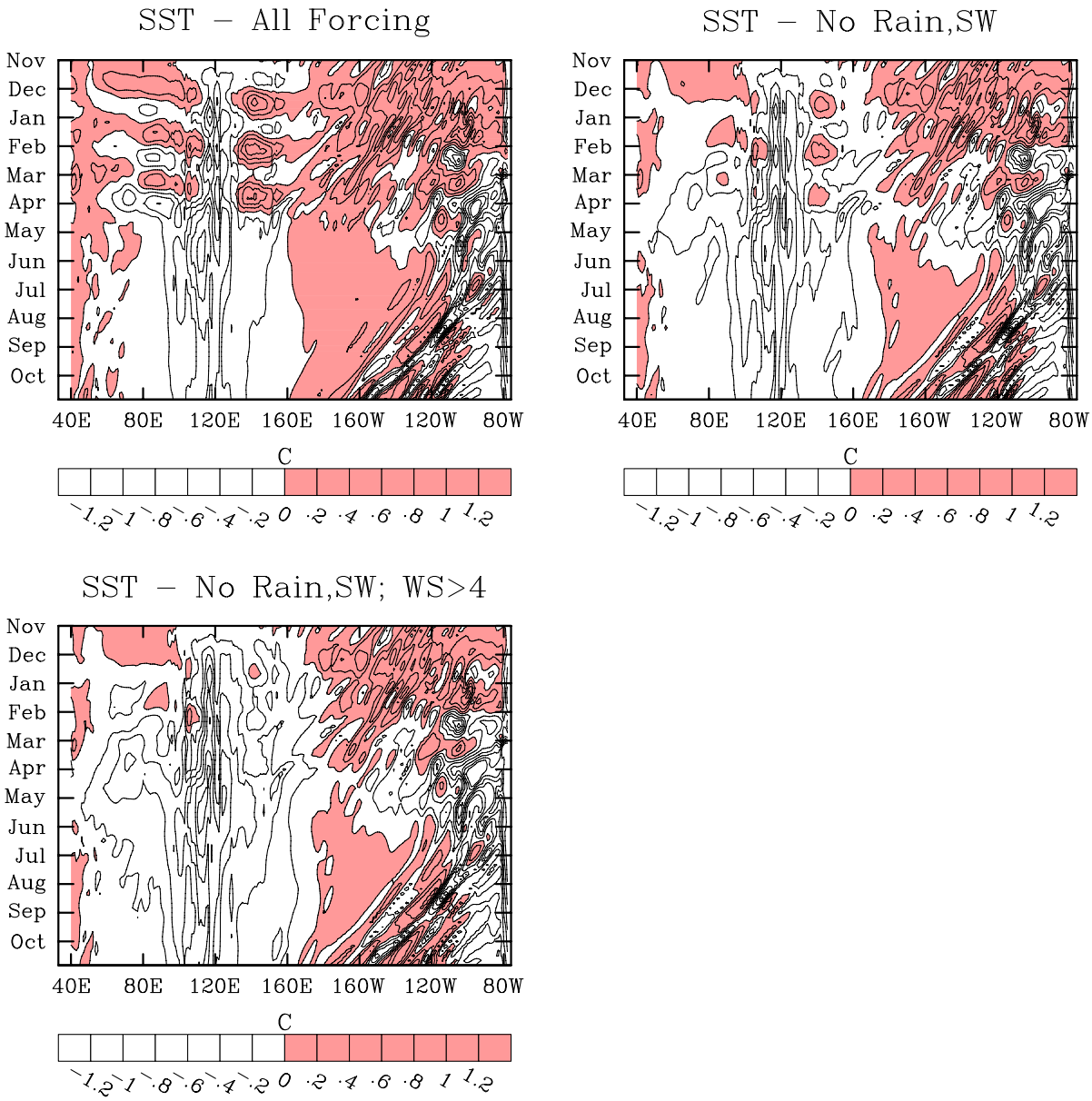

Figure 2. Equatorial (5N-5S) time-longitude diagrams of the difference in the ocean model sea surface temperature response between cases which include intraseasonal forcing to the case with climatological forcing alone: (upper left) all intraseasonal forcing components (i.e. Fig. 1), (upper right) no rainfall or shortwave intraseasonal forcing, (lower left) no rainfall or shortwave intraseasonal forcing as well as the application of an absolute minimum value for surface wind speed (>= 4m/s).